^{77}Se Solid-State NMR Spectroscopy and Structures of Tetramethylammonium Pentaselenide and Hexaselenide Complexes

Patrick J. Barrie and Robin J. H. Clark*

Department of Chemistry, Christopher Ingold Laboratories, University College London, 20 Gordon Street, London WC1H 0AJ, U.K.

Duck-Young Chung, Debojit Chakrabarty, and Mercouri G. Kanatzidis

Department of Chemistry, Michigan State University, East Lansing, Michigan 48824

Received February 3, 1995[⊗]

High-resolution ^{77}Se solid-state NMR spectra are reported for $[NMe_4]_2Se_5$ and $[NMe_4]_2Se_6$. The isotropic chemical shifts for the former are similar to those observed for the Se_5^{2-} ion in solution, suggesting that the conformation adopted by the anion is similar in the solid state and solution. The agreement between the chemical shifts for the Se_6^{2-} anion in the solid state and solution is less good. The spectra show that the five selenium sites are distinct in $[NMe_4]_2Se_5$ while the symmetry of $[NMe_4]_2Se_6$ is such that there are only three crystallographically different selenium sites. Single-crystal X-ray structure determinations of $[NMe_4]_2Se_5$ and $[NMe_4]_2Se_6$ are reported which are consistent with this observation. Using α, β, and γ to signify the selenium atom positions relative to the ends of the chain, the shielding anisotropies for the α and β sites are large (in the range 720–1175 ppm), while those for the γ sites are lower than these (614 and 332 ppm).

Much research has recently been devoted to the synthesis of a wide range of novel polyselenide and polytelluride complexes.[1-4] Thus far, characterization of these complexes has depended principally on single-crystal X-ray diffraction studies, though there has been a certain amount of ^{77}Se/^{125}Te NMR work on these species in solution[4,5] and a solid-state NMR spectrum of $[NMe_4]_2Te_2$ has also been reported.[6] For instance, the trends in ^{77}Se chemical shifts for Se_x^{2-} anions in solution ($x = 1-6$) have been explored.[7,8] However, attempts to observe Se_5^{2-} and Se_6^{2-} anions in solution using ^{77}Se NMR fail at room temperature due to exchange broadening of the lines.[7,8] Reducing the temperature to 230 K can lead to the detection of successful spectra,[7] though in some solvents there are problems associated with low solubility.[8] Solid-state NMR spectra do not normally suffer from these complications and have the added advantage that they can provide a measurement of the anisotropy of the shielding tensor; thus solid-state NMR spectroscopy is expected to be a highly sensitive probe of detailed structural geometry. While solid-state NMR of less common spin-$^1/_2$ nuclei such as ^{77}Se is still in the stage of "mostly qualitative usage of isotropic chemical shifts and/or chemical shift anisotropies",[9] there is a growing number of *ab initio* calculations of ^{77}Se NMR parameters which begin to approach experimentally determined values.[10,11] In a previous publication we reported the first solid-state ^{77}Se NMR results on polyselenide complexes.[12] The spectra of $[M(Se_4)_2]^{2-}$ complexes (M = Zn, Cd, or Hg) demonstrated the viability of this technique for obtaining structural information. In this work we report ^{77}Se solid-state NMR results on $[NMe_4]_2Se_5$ and $[NMe_4]_2Se_6$ which, as model compounds, extend the likelihood of obtaining useful information on new polychalcogenide solids. The selenide anions in these complexes are open chains and, for convenience, the selenium atom positions relative to the ends of the chain are denoted by α, β, and γ. The spectra reveal the number of selenium crystallographic sites present; the chemical shifts are compared with those obtained on the anions in solution, and the principal components of the shielding tensor are determined. Any discussion of solid-state NMR spectra needs to take into account the detailed structure of the solid and, for this reason, single-crystal X-ray structure determinations of $[NMe_4]_2Se_5$ and $[NMe_4]_2Se_6$ are also reported.

Experimental Section

Starting Materials. The chemicals in this research were used as obtained commercially: selenium, 99.5+% purity, Aldrich Chemical Co. Inc., Milwaukee, WI; potassium metal, analytical reagent, Mallinckrodt Inc., Paris, KY; tetramethylammonium chloride, 98+% purity, Lancaster Synthesis Inc., Windham, NH. Dimethylformamide (DMF, analytical reagent) was stored over 4A Linde molecular sieves for over 1 week and then distilled under reduced pressure at 25–30 °C. The first 50 cm^3 was discarded. Diethyl ether (ACS anhydrous, Columbus Chemical Industries Inc., Columbus, WI) was distilled after being held under reflux with potassium in the presence of benzophenone and triethylene glycol dimethyl ether for 4 h. K_2Se_2, K_2Se_4, and K_2Se_5 were prepared by using stoichiometric amounts of elemental K and Se in liquid ammonia. $K_3[Mn(CN)_6]$ was

[⊗] Abstract published in *Advance ACS Abstracts,* July 15, 1995.

(1) Roof, L. C.; Kolis, J. W. *Chem. Rev.* **1993**, *93*, 1037.
(2) Kanatzidis, M. G.; Huang, S.-P. *Coord. Chem. Rev.* **1994**, *130*, 509.
(3) Ansari, M. A.; McConnachie, J. M.; Ibers, J. A. *Acc. Chem. Res.* **1993**, *26*, 574.
(4) Ansari, M. A.; Ibers, J. A. *Coord. Chem. Rev.* **1990**, *100*, 223.
(5) Duddeck, H. *Prog. NMR Spectrosc.* **1995**, *27*, 1.
(6) Batchelor, R. J.; Einstein, F. W. B.; Gay, I. D.; Jones, C. H. W.; Sharma, R. D. *Inorg. Chem.* **1993**, *32*, 4378.
(7) Björgvinsson, M.; Schrobilgen, G. J. *Inorg. Chem.* **1991**, *30*, 2540.
(8) Cusick, J.; Dance, I. *Polyhedron* **1991**, *10*, 2629.
(9) Sebald, A., Solid-State NMR II. In *NMR*; Diehl, P., Fluck, E., Günther, H., Kosfeld, R., Seelig, J., Eds.; Springer: Berlin, 1994; Vol. 31, 91.
(10) Ellis, P. D.; Odom, J. D.; Lipton, A. S.; Chen, Q.; Gulick, J. M. *Nuclear Magnetic Shieldings and Molecular Structure*; NATO ASI Series; Kluwer: Dordrecht, The Netherlands, 1993; Vol. *C386*, p 539.
(11) Magyarfalvi, G.; Pulay, P. *Chem. Phys. Lett.* **1994**, *225*, 280.
(12) Barrie, P. J.; Clark, R. J. H.; Withnall, R.; Chung, D.-Y.; Kim, K.-W.; Kanatzidis, M. G. *Inorg. Chem.* **1994**, *33*, 1212.

0020-1669/95/1334-4299$09.00/0

prepared as described elsewhere.[13] All syntheses were performed under an atmosphere of dry nitrogen in a Vacuum Atmospheres Dri-Lab glovebox or in a Schlenk line.

Synthesis of $[Me_4N]_2Se_5$. A 0.26 g (2.54 mmol) amount of $[Me_4N]Cl$ in 60 cm^3 of DMF was stirred overnight and 0.5 g (1.15 mmol) of K_2Se_5 was added. The mixture was filtered after being stirred for 2 h. The dark green filtrate was carefully layered with 100 cm^3 of diethyl ether and allowed to stand for 2 days. The black needlelike crystals were isolated in near-quantitative yield and washed several times with diethyl ether.

Synthesis of $[Me_4N]_2Se_6$. Three preparative routes were successful:

Method A. To the suspension of 0.5 g (4.56 mmol) of $[Me_4N]Cl$ in 30 cm^3 of ethylenediamine was added 0.87 g (2.21 mmol) of K_2Se_4 and 0.35 g (4.43 mmol) of Se. The mixture was stirred for 1 day to complete the reaction. Black precipitates were filtered out and dissolved in 20 cm^3 of DMF. Following filtration, 100 cm^3 of diethyl ether was layered over the dark green filtrate to incipient crystallization. Upon being allowed to stand at room temperature for 1 week, black platelets of $[Me_4N]_2Se_6$ were formed and isolated by filtration. These crystals were used for the ^{77}Se solid-state NMR studies after recrystallization from DMF−diethyl ether. The overall yield was 47% based on K_2Se_4.

Method B. A 0.32 g (1.36 mmol) amount of K_2Se_2, 0.43 g (5.45 mmol) of Se, 0.30 g (2.74 mmol) of $[Me_4N]Cl$, and 0.15 g (0.46 mmol) of $K_3[Mn(CN)_6]$ were mixed in 20 cm^3 of DMF and stirred for 1 day. The resulting solution was filtered, and 60 cm^3 diethyl ether was slowly added to the dark green filtrate. After being allowed to stand for 4 days, black crystals were isolated and washed several times with diethyl ether. The yield was 75% based on K_2Se_2.

Method C. The mixture of 0.40 g (1.02 mmol) of K_2Se_4, 0.32 g (4.06 mmol) of Se, and 0.23 g (2.10 mmol) of $[Me_4N]Cl$ in 30 cm^3 of DMF was stirred overnight at ice-water temperature and then filtered to remove KCl. A 100 cm^3 volume of cold diethyl ether was slowly layered over the filtrate solution and allowed to stand for a week in a refrigerator to give black crystals. These crystals were isolated and washed with diethyl ether several times. The yield was 79% based on K_2Se_4.

Crystallography. A single crystal of $[Me_4N]_2Se_5$ was mounted on the tip of a glass fiber and covered with glue. A single crystal of $[Me_4N]_2Se_6$ was placed inside a glass capillary and flame-sealed. The crystallographic data for both crystals were collected on a Rigaku AFC6S four-circle automated diffractometer at room temperature. Accurate unit cell parameters were determined from the 2θ, ω, and χ angles of 22 and 23 machine-centered reflections for $[Me_4N]_2Se_5$ and $[Me_4N]_2Se_6$, respectively. The intensities of three standard reflections were checked every 150 reflections to monitor crystal and instrument stability. An empirical absorption correction based on ψ scans of three strong reflections with $\chi \sim 90°$ was applied to the data set. The structures were solved by direct methods using the SHELXS-86 software program and refined with full-matrix least-squares techniques. After isotropic refinement of all atoms, a DIFABS correction was applied.[14] All calculations were performed on a VAX station 3100/76 computer using TEXSAN crystallographic software package of the Molecular Structure Corp.[15] All Se atoms of $[Me_4N]_2Se_5$ were refined anisotropically and the C and N atoms of the $[Me_4N]^+$ cations were refined as a rigid group. For $[Me_4N]_2Se_6$, all non-hydrogen atoms were refined anisotropically. The hydrogen atom positions in both compounds were calculated but not refined. Table 1 shows the crystal data and details of the structure analysis. The fractional coordinates and temperature factors (B_{eq}) of all non-hydrogen atoms together with their estimated standard deviations are given in Tables 2 and 3.

Solid-State NMR. The ^{77}Se solid-state NMR spectra were recorded at 57.24 MHz using a multinuclear Bruker MSL-300 spectrometer using magic-angle spinning (MAS) and high-power proton decoupling. For the $[NMe_4]_2Se_5$ complex, a good quality spectrum was achieved using cross-polarization (CP) with a 12

(13) Lower, J. A.; Fernelius, W. C. *Inorg. Synth.* **1946**, *2*, 213.
(14) Walker, N.; Stuart, D. DIFABS: An Empirical Method for Correcting Diffractometer Data for Absorption Effects. *Acta Crystallogr.* **1983**, *A39*, 158.
(15) TEXSAN: Single Crystal Structure Analysis Software, Version 5.0, Molecular Structure Corp., The Woodlands, TX.

Table 1. Crystallographic Data for $[Me_4N]_2Se_5$ and $[Me_4N]_2Se_6$

formula	$C_8H_{24}N_2Se_5$	$C_8H_{24}N_2Se_6$
fw	543.09	622.05
crystal size, mm	0.51 × 0.12 × 0.18	0.52 × 0.26 × 0.01
a, Å	13.084(6)	7.547(2)
b, Å	19.565(6)	5.818(4)
c, Å	7.046(2)	21.779(4)
β, deg	90.0	96.31(2)
V, Å^3	1804(1)	951(1)
Z	4	2
space group	$P2_12_12_1$ (No. 19)	$P2/c$ (No. 13)
temp, °C	23	23
λ, Å (Mo Kα)	0.710 69	0.710 69
μ, cm^{-1}	100.35	114.19
ϱ_{calcd}, g cm^{-3}	2.000	2.173
$R(F_o)^a$	0.060	0.065
$R_w(F_o)^b$	0.064	0.080

$^a R = \sum||F_o| - |F_c||/\sum|F_o|$. $^b R_w = \{\sum w(|F_o| - |F_c|)^2/\sum w|F_o|^2\}^{1/2}$.

Table 2. Fractional Atomic Coordinates and B_{eq} Values for Non-Hydrogen Atoms in $[Me_4N]_2Se_5$ with Their Estimated Standard Deviations in Parentheses

$[Me_4N]_2Se_5$	x	y	z	$B_{eq}{}^a$
Se(1)	0.6638(5)	0.1350(3)	−0.4012(7)	5.8(3)
Se(2)	0.7308(5)	0.1712(3)	−0.1165(8)	6.0(4)
Se(3)	0.6022(5)	0.2221(3)	0.0637(7)	5.6(3)
Se(4)	0.5490(5)	0.3244(3)	−0.0795(7)	4.9(3)
Se(5)	0.6650(5)	0.4118(2)	−0.0380(6)	4.8(3)
N(1)	0.333(2)	0.1681(9)	−0.452(2)	6.0(6)
N(2)	0.547(2)	−0.028(1)	0.053(3)	7.6(7)
C(1)	0.223(2)	0.179(2)	−0.480(4)	6.0(6)
C(2)	0.390(3)	0.195(2)	−0.616(4)	6.0(6)
C(3)	0.354(3)	0.095(1)	−0.430(5)	6.0(6)
C(4)	0.366(3)	0.204(2)	−0.279(4)	6.0(6)
C(5)	0.605(3)	−0.019(2)	−0.124(4)	7.6(7)
C(6)	0.448(2)	0.007(2)	0.036(5)	7.6(7)
C(7)	0.604(3)	0.002(2)	0.212(4)	7.6(7)
C(8)	0.530(3)	−0.101(1)	0.087(5)	7.6(7)

^{a} Anisotropically refined atoms are given in the form of the isotropic equivalent displacement parameter defined as $B_{eq} = (8\pi^2/3)[a^2B_{11} + b^2B_{22} + c^2B_{33} + ab(\cos\gamma)B_{12} + ac(\cos\beta)B_{13} + bc(\cos\alpha)B_{23}]$. The anisotropic temperature factor expression is $\exp[-2\pi^2(B_{11}a^{*2}h^2 + ... + 2B_{12}a^*b^*hk + ...)]$.

Table 3. Fractional Atomic Coordinates and B_{eq} Values (Å^2) for Non-Hydrogen Atoms in $[Me_4N]_2Se_6$ with Their Estimated Standard Deviations in Parentheses

$[Me_4N]_2Se_6$	x	y	z	$B_{eq}{}^a$
Se(1)	0.7179(3)	0.3972(4)	0.4233(1)	3.0(1)
Se(2)	0.7174(3)	0.3200(5)	0.3195(1)	4.1(1)
Se(3)	0.6574(4)	0.6545(6)	0.2633(1)	6.6(2)
N(1)	0.776(2)	0.000(3)	0.0955(8)	2.5(8)
C(1)	0.779(3)	0.145(4)	0.1523(9)	3(1)
C(2)	0.612(3)	−0.147(4)	0.088(1)	4(1)
C(3)	0.780(3)	0.152(4)	0.041(1)	4(1)
C(4)	0.939(3)	−0.153(4)	0.101(1)	4(1)

^{a} B_{eq} is defined as in the footnote to Table 2.

Table 4. ^{77}Se Shielding Tensor Results on $[NMe_4]_2Se_5$[a]

site	δ_{iso}, ppm	σ_{11}, ppm	σ_{22}, ppm	σ_{33}, ppm	$\Delta\sigma$, ppm	η	Ω, ppm	κ
Se(γ)	864	−1218(±15)	−920(±13)	−455(±12)	614	0.73	763	0.22
Se(β_1)[b]	567	−999(±44)	−884(±31)	185(±15)	1126	0.15	1184	0.81
Se(β_2)[b]	564							
Se(α_1)	389	−629(±33)	−629(±30)	91(±11)	720	0.0	720	1.00
Se(α_2)	366	−661(±45)	−661(±39)	224(±19)	885	0.0	885	1.00

[a] The shielding tensor components, σ, have the opposite sign to chemical shifts, δ, and are quoted using the convention $\sigma_{11} \leq \sigma_{22} \leq \sigma_{33}$. The other parameters given are the anisotropy, $\Delta\sigma$, defined as $\sigma_{33} - 0.5(\sigma_{11} + \sigma_{22})$; the asymmetry parameter, η, defined as $(\sigma_{22} - \sigma_{11})/(\sigma_{33} - \sigma_{iso})$; the span, Ω, defined as $\sigma_{33} - \sigma_{11}$; and the skew, κ, defined as $3(\sigma_{iso} - \sigma_{22})/\Omega$.[19] The isotropic chemical shifts are accurate within ±2 ppm. [b] Due to the overlap between the peaks for the Se(β_1) and Se(β_2) sites, the shielding tensor components given here were obtained by simulating the combined peak.

ms mixing time and a recycle delay of 0.25 s. The $[NMe_4]_2Se_6$ complex did not give a good quality CP spectrum but gave an acceptable spectrum using single pulse excitation with a recycle delay between scans of 15 s. The spectra were recorded using three different spinning speeds in the range 6-10 kHz in order to identify unambiguously the isotropic resonance positions. Chemical shifts are quoted relative to Me_2Se by employing solid ammonium selenate as an external secondary reference taken to resonate at 1040.2 ppm.[16] Spinning sideband intensities were simulated using an iterative fit program based on the method of Herzfeld and Berger to give the principal components of the shielding tensor (σ_{11}, σ_{22}, and σ_{33}).[17,18] There are a confusing number of different conventions for reporting shielding tensor information; in this paper we quote the span and the skew according to the recent proposal of Mason designed to clarify the situation,[19] and we also quote the anisotropy and asymmetry parameter according to Haeberlen's convention[20] to allow easy comparison with existing data in the literature. Definitions of these parameters are given in the footnote to Table 4.

Powder Diffraction. The purity of the bulk samples used for the solid-state NMR experiments was checked using powder X-ray diffraction, both in Michigan State University (Rigaku-Denki/RW400F2, Rotaflex) and UCL (Siemens D5000 diffractometer).

Results

Figure 1 shows ^{77}Se solid-state NMR spectra of $[NMe_4]_2Se_5$ and $[NMe_4]_2Se_6$. The isotropic peaks are marked with arrows, while the other peaks are spinning sidebands. Five isotropic peaks are identified for $[NMe_4]_2Se_5$, implying that the five selenium atoms in the anion are unrelated by symmetry and so crystallographically distinct. This is not unexpected considering the reported crystal structures of Se_5^{2-} complexes with Rb^+, Cs^+, and $[PPh_4]^+$,[21-23] though there is a mirror plane in the cesium−18-crown-6 complex which renders the two α and β selenium sites equivalent in this case.[24] It should be noted that resolution of the two Se(β) sites requires very accurate setting of the magic angle. The shielding tensor results obtained from analysing the spinning sideband intensities are presented in Table 4. By contrast to the situation for $[NMe_4]_2Se_5$, only three

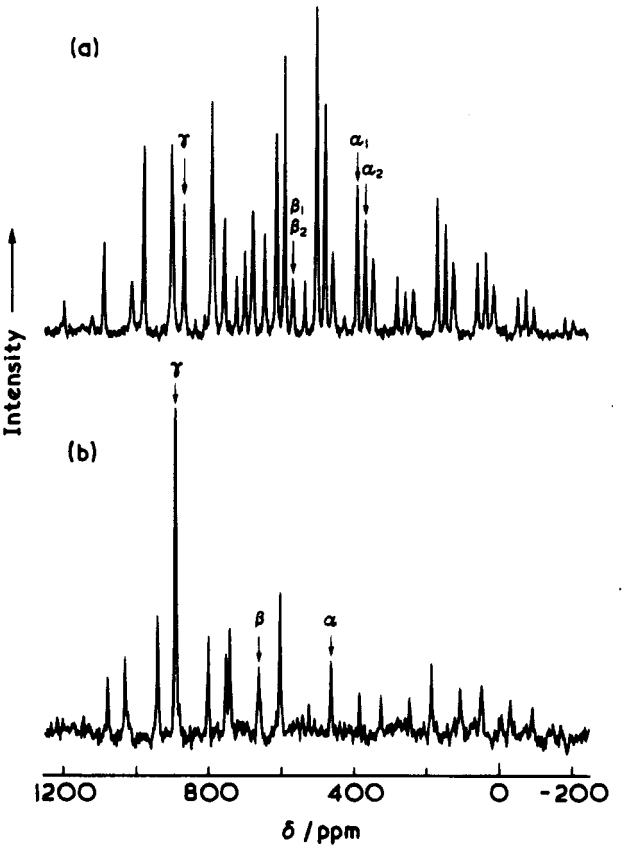

Figure 1. ^{77}Se MAS NMR spectra of (a) $[NMe_4]_2Se_5$ recorded with CP at a spinning speed of 6325 Hz and (b) $[NMe_4]_2Se_6$ recorded without CP at 7940 Hz. The isotropic peaks are marked by arrows, while the other peaks are spinning sidebands.

selenium sites are detected for $[NMe_4]_2Se_6$ implying that there must be symmetry within the anion (Table 5). Two previous crystal structure determinations of Se_6^{2-} complexes have shown the presence of a 2-fold symmetry axis which would account for the NMR observation;[25,26] on the other hand all the six selenium sites are crystallographically distinct in the crystal structure of $[PPh_4]_2Se_6$.[27]

In order to establish the anion symmetry, single-crystal X-ray structure refinements were performed on both $[NMe_4]_2Se_5$ and $[NMe_4]_2Se_6$ (Tables 1−3, Figures 2−5). The space group for $[NMe_4]_2Se_5$ is $P2_12_12_1$, and thus there are five crystallographically distinct Se sites. The space group for $[NMe_4]_2Se_6$ is $P2/c$ with the center of symmetry located between the two central selenium atoms of the Se_6^{2-} anion giving three crystallographi-

(16) Collins, M. J.; Ratcliffe, C. I.; Ripmeester, J. A. *J. Magn. Reson.* **1986**, *68*, 172.
(17) Herzfeld, J.; Berger, A. E. *J. Chem. Phys.* **1980**, *73*, 6021.
(18) Hawkes, G. E.; Sales, K. D.; Lian, L. Y.; Gobetto, R. *Proc. R. Soc. London A* **1989**, *424*, 93.
(19) Mason, J. *Solid State Nucl. Magn. Reson.* **1993**, *2*, 285.
(20) Haeberlen, U. High Resolution NMR in Solids: Selective Averaging. *Adv. Magn. Reson. Suppl. 1*, **1976**, 9.
(21) Böttcher, P. *Z. Kristallogr.* **1979**, *150*, 65.
(22) Kretschmann, U.; Böttcher, P. *Z. Naturforsch.* **1985**, *40b*, 895.
(23) Chau, C.-N.; Wardle, R. W. M.; Ibers, J. A. *Acta Crystallogr.* **1988**, *C44*, 883.
(24) Brese, N. E.; Randall, C. R.; Ibers, J. A. *Inorg. Chem.* **1988**, *27*, 940.
(25) Teller, R. G.; Krause, L. J.; Haushalter, R. C. *Inorg. Chem.* **1983**, *22*, 1809.
(26) Weller, F.; Adel, J.; Dehnicke, K. *Z. Anorg. Allg. Chem.* **1987**, *548*, 125.
(27) Fenske, D.; Kraus, C.; Dehnicke, K. *Z. Anorg. Allg. Chem.* **1992**, *607*, 109.

Table 5. ^{77}Se Shielding Tensor Results on $[NMe_4]_2Se_6$[a]

site	δ_{iso}, ppm	σ_{11}, ppm	σ_{22}, ppm	σ_{33}, ppm	$\Delta\sigma$, ppm	η	Ω, ppm	κ
Se(γ)[b]	890				332(±50)			
Se(β)	662	−1190(±31)	−917(±24)	121(±27)	1175	0.35	1311	0.58
Se(α)	463	−904(±32)	−654(±31)	169(±29)	947	0.40	1073	0.53

[a] See the footnote to Table 4 for definitions. [b] The anisotropy for Se(γ) is such that insufficient spinning sidebands were obtained at the spinning speeds used to provide anything other than an approximate measurement of $\Delta\sigma$.

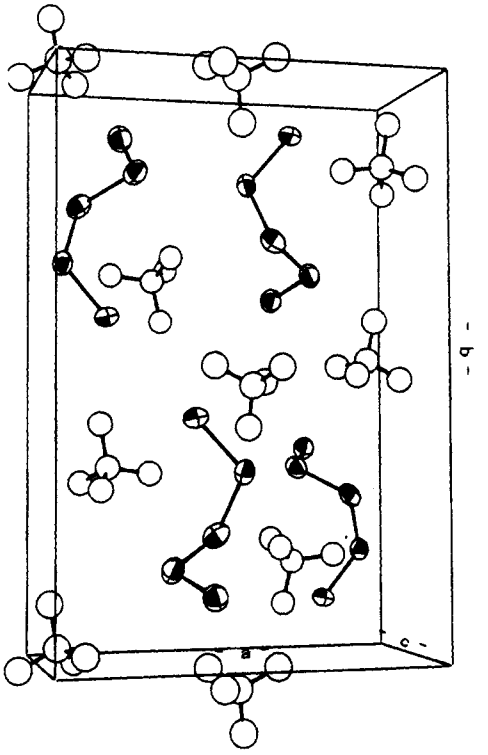

Figure 2. Packing diagram of the unit cell of $[NMe_4]_2Se_5$.

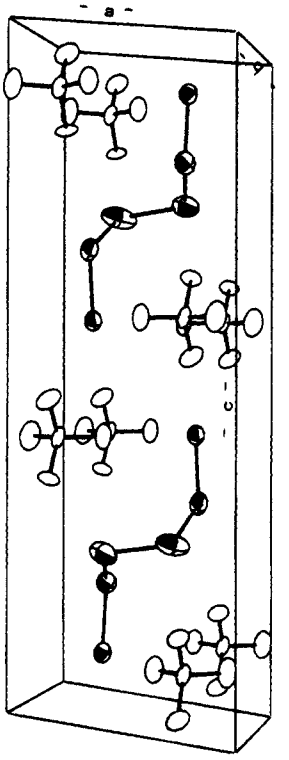

Figure 3. Packing diagram of the unit cell of $[NMe_4]_2Se_6$.

cally distinct Se sites. The NMR observations are thus in agreement with the diffraction results.

It is interesting to note that the isotropic chemical shifts of $[NMe_4]_2Se_6$ correspond exactly with those of the impurity phase detected in the sample of $[NMe_4]_2Zn(Se_4)_2$ reported by us previously.[12] Identification of the impurity to be $[NMe_4]_2Se_6$ on this basis provides a nice demonstration of the analytical power of the technique. It is also worth commenting that $[NMe_4]_2Se_6$ suffers partial decomposition on exposure to air giving elemental selenium and an amorphous phase with ^{77}Se NMR peaks at 1393 and 794 ppm.

Unfortunately no $^1J(^{77}Se-^{77}Se)$ coupling satellites are observed for either sample. This is primarily because the line widths ($\Delta\nu_{1/2}$ = 120−180 Hz) are of the same magnitude as the expected coupling constants (130-180 Hz).[7,12] In any case, the natural abundance of ^{77}Se is only 7.6%, and so $^1J(^{77}Se-^{77}Se)$ coupling satellites can be difficult to detect even when line widths are small.

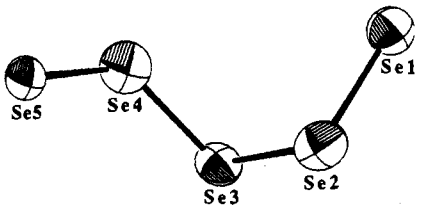

Figure 4. Structure of the Se_5^{2-} anion in $[NMe_4]_2Se_5$.

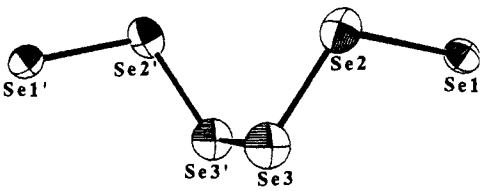

Figure 5. Structure of the Se_6^{2-} anion in $[NMe_4]_2Se_6$.

Discussion

Our previous solid-state NMR work on $[M(Se_4)_2]^{2-}$ complexes indicated that the exact geometry of the metal−polyselenide anion depends to some extent on the cation present.[12] The crystal structure determinations of $[NMe_4]_2Se_5$ and $[NMe_4]_2Se_6$ reported in this work may be compared with those of Se_5^{2-} and Se_6^{2-} complexes with other cations.[21-27] This forms part of an investigation into the interaction between the ions in these complexes and the conformational changes in the solid state which can occur as a result of varying packing forces. For example, the crystal packing in the structure of $[Ph_4P]_2Se_5$ requires that the anion sits on a special position[23] and thus the free helical structure found for $[Me_4N]_2Se_5$ cannot be adopted in this case. While the Se_5^{2-} anion lies on a general position for $[Me_4N]_2Se_5$, the Se_6^{2-} anion in $[Me_4N]_2Se_6$ sits on a crystallographic inversion center. The structures of both Se_5^{2-} and Se_6^{2-} anions have the expected helical-fragment conformation (Figures 4 and 5) as has been seen several times in previous determinations involving other organic counterions.[23-27] One characteristic feature of the structure of the polychalcogenide Se_x^{2-} anions is that the two terminal Se−Se bonds are shorter than those bonds involving internal selenium atoms; this is

Table 6. Selected Bond Distances (Å), Angles (deg), and Torsion Angles (deg) for Se_5^{2-} and Se_6^{2-} in $[Me_4N]^+$ and $[Ph_4P]^+$ Salts

	$[Me_4N]_2Se_5$	$[Ph_4P]_2Se_5$[a]	$[Me_4N]_2Se_6$[b]	$[Ph_4P]_2Se_6$[c]
Se(1)−Se(2)	2.301(8)	2.316(2)	2.304(4)	2.293(2)
Se(2)−Se(3)	2.331(9)	2.355(2)	2.317(4)	2.314(2)
Se(3)−Se(4)	2.348(7)	2.366(2)		2.355(2)
Se(4)−Se(5)	2.305(8)	2.314(2)		2.313(2)
Se(5)−Se(6)				2.285(2)
Se(3)−Se(3′)			2.383(6)	
Se(1)−Se(2)−Se(3)	109.3(3)	108.83(6)	109.5(1)	109.20(7)
Se(2)−Se(3)−Se(4)	110.1(3)	110.59(7)		105.26(7)
Se(3)−Se(4)−Se(5)	112.5(3)	109.02(6)		105.93(7)
Se(4)−Se(5)−Se(6)				110.03(7)
Se(2)−Se(3)−Se(3′)			105.1(1)	
Se(1)−Se(2)−Se(3)−Se(4)	−67.5(4)	77.32(8)		−81.19(8)
Se(2)−Se(3)−Se(4)−Se(5)	−75.2(4)	89.16(7)		−71.54(8)
Se(3)−Se(4)−Se(5)−Se(6)				−76.37(8)
Se(1)−Se(2)−Se(3)−Se(3′)			−92.9(2)	
Se(2)−Se(3)−Se(3′)−Se(2′)			−59.0(3)	

[a] Reference 23; note that this refinement was performed on data recorded at 123 K. [b] Anion sits on a center of symmetry. [c] Reference 27; note that this refinement was performed on data recorded at 200 K.

Table 7. Selected Short Distances (<3.35 Å) between Se and H Atoms in $[Me_4N]_2Se_5$

Se(1)−H(15)	2.818	Se(4)−H(22)	3.034
Se(1)−H(1)	2.906	Se(4)−H(2)	3.096
Se(1)−H(24)	3.175	Se(4)−H(23)	3.104
Se(1)−H(4)	3.186	Se(4)−H(10)	3.149
Se(1)−H(13)	3.223	Se(4)−H(11)	3.319
Se(1)−H(19)	3.223	Se(5)−H(2)	2.954
Se(1)−H(9)	3.238	Se(5)−H(8)	3.154
Se(2)−H(6)	3.094	Se(5)−H(22)	3.165
Se(2)−H(15)	3.181	Se(5)−H(3)	3.224
Se(2)−H(24)	3.192	Se(5)−H(12)	3.251
Se(3)−H(4)	3.096	Se(5)−H(7)	3.251
Se(3)−H(10)	3.187	Se(5)−H(17)	3.327

Table 8. Selected Short Distances (<3.35 Å) between Se and H Atoms in $[Me_4N]_2Se_6$

Se(1)−H(4)	3.122	Se(1)−H(11)	3.322
Se(1)−H(7)	3.128	Se(1)−H(3)	3.344
Se(1)−H(5)	3.141	Se(2)−H(2)	3.029
Se(1)−H(8)	3.203	Se(2)−H(3)	3.170
Se(1)−H(9)	3.258	Se(2)−H(12)	3.185
Se(1)−H(6)	3.314	Se(3)−H(1)	3.021
Se(1)−H(9)	3.317	Se(3)−H(6)	3.100
Se(1)−H(12)	3.319		

thought to be due to partial $p_\pi-d_\pi$ bonding. Table 6 compares structural parameters of $[Me_4N]_2Se_5$ and $[Me_4N]_2Se_6$ with those of the $[PPh_4]^+$ analogues. It can be seen that the bond lengths are slightly different and that there are significant differences in bond angles and torsion angles. For instance, the bond length between the two central Se(γ) sites is 2.383 Å in $[Me_4N]_2Se_6$ compared to 2.355 Å in $[Ph_4P]_2Se_6$. It is interesting to note that the internal Se(2)−Se(3)−Se(4) bond angle for $[Me_4N]_2Se_5$ and $[Ph_4P]_2Se_5$ is similar (110.1 and 110.6°, respectively); this angle is significantly larger than those found for other Se_5^{2-} complexes for which structures are known (104.5−106.6°).[21-24]

The structure determinations are also useful in providing the Se−H contacts that are responsible for the magnetization transfer during the CP NMR experiment. The distances between the selenium sites and the nearest calculated hydrogen atom positions in $[Me_4N]_2Se_5$ and $[Me_4N]_2Se_6$ are given in Tables 7 and 8. All selenium sites have several hydrogen atoms within the range 2.8-3.35 Å, with the two terminal, negatively-charged, atoms of the Se_5^{2-} and Se_6^{2-} anions having the most nearby hydrogen atoms. While distances of about 3 Å are fairly long for CP, they are still short enough for reasonable magnetization transfer to occur unless the $T_{1\varrho}$ relaxation times are small. However, magnetization transfer from methyl groups, when employing MAS at rates comparable to the magnitude of the ^1H homonuclear dipolar coupling, is handicapped by the Hartmann−Hahn match condition splitting up into a series of sharp sidebands.[28] This property, together with the fairly long Se−H distances, means that the efficiency of magnetization transfer becomes extremely sensitive to the exact setting of the power levels, spinning speed stability, and any amplifier drift.[28] It may well be for this reason, rather than as a result of unfavorable relaxation effects, that a good-quality CP spectrum for $[Me_4N]_2Se_6$ could not be obtained.

It is interesting to compare the ^{77}Se isotropic chemical shifts of $[Me_4N]_2Se_5$ and $[Me_4N]_2Se_6$ with those observed for Se_5^{2-} and Se_6^{2-} in mixed DMF/ethanol solutions at 230 K. The α, β, and γ sites give rise to signals at 354, 570, and 868 ppm, respectively, for Se_5^{2-} in solution, and at 404, 636, and 807 ppm for Se_6^{2-} in solution.[8] It should be noted, however, that the ^{77}Se chemical shifts in solution are very dependent on solvent proticity, particularly those of the terminal, Se(α), sites.[8] The close similarity of the Se(γ) and Se(β) chemical shifts for Se_5^{2-} in solution to those observed in the solid state is surprising, an observation which suggests that the conformation adopted by the anion in each state is probably very similar. On the other hand, the agreement between the chemical shifts for Se_6^{2-} is less good; while the differences in observed chemical shifts of the Se(α) and Se(β) sites can be explained by solvent effects, the significant change in chemical shift of the Se(γ) site probably indicates that the conformation of Se_6^{2-} in solution and in solid $[Me_4N]_2Se_6$ is different. As observed in solution, there is a general trend that $\delta_{Se(\gamma)} > \delta_{Se(\beta)} > \delta_{Se(\alpha)}$ which is associated with increasing distance from the end of the chain where the negative charge density is the greatest. Also the chemical shifts for Se_6^{2-} are at higher frequency than those for Se_5^{2-}; this may be ascribed to a reduction in overall negative charge density. This is true for all the sites measured here; the fact that the chemical shifts of the Se(γ) sites for Se_5^{2-} and Se_6^{2-} in DMF/ethanol solution are the other way around from that expected may be viewed as an anomaly.

The chemical shift anisotropies are very large for the Se(β) sites and slightly less for the Se(α) sites (Tables 4 and 5). We found anisotropies of comparable magnitude previously for $[M(Se_4)_2]^{2-}$ complexes.[12] Interestingly, the symmetry of the shielding tensor is axial or very close to axial for the Se(α) and Se(β) sites in $[NMe_4]_2Se_5$ but further away from axial for $[NMe_4]_2Se_6$. A significant observation is that the Se(γ) sites have a lower anisotropy than the other sites. Indeed, the

(28) Kolbert, A. C; Gann, S. L. *Chem. Phys. Lett.* **1994**, *224*, 86.

anisotropy for the Se(γ) site in $[NMe_4]_2Se_6$ is so low that insufficient spinning sidebands were obtained at the spinning speeds used to provide anything other than an approximate measurement of $\Delta\sigma$. It is as yet unclear why the anisotropy of this site is lower than those of the others, but it may reflect the longer Se−Se bond distances at this site or the unusual Se−Se−Se bond angle.

Acknowledgment. We thank the University of London Intercollegiate Research Services (ULIRS) for provision of solid-state NMR facilities. Financial support from the Petroleum Chemical Research Fund, administered by the American Chemical Society, and the National Science Foundation Grant CHE-8958451 is gratefully acknowledged.

Supporting Information Available: Tables of crystal data and anisotropic thermal parameters (3 pages). Ordering information is given on any current masthead page.

IC950120L